


RESEARCH ARTICLE

Open Access



Transcriptome analyses of 7-day-old zebrafish larvae possessing a familial Alzheimer's disease-like mutation in *psen1* indicate effects on oxidative phosphorylation, ECM and MCM functions, and iron homeostasis

Yang Dong¹, Morgan Newman¹, Stephen M. Pederson², Karissa Barthelson¹, Nhi Hin^{1,2} and Michael Lardelli^{1*} 

Abstract

Background: Early-onset familial Alzheimer's disease (EOfAD) is promoted by dominant mutations, enabling the study of Alzheimer's disease (AD) pathogenic mechanisms through generation of EOfAD-like mutations in animal models. In a previous study, we generated an EOfAD-like mutation, *psen1*^{Q96_K97del}, in zebrafish and performed transcriptome analysis comparing entire brains from 6-month-old wild type and heterozygous mutant fish. We identified predicted effects on mitochondrial function and endolysosomal acidification. Here we aimed to determine whether similar effects occur in 7 day post fertilization (dpf) zebrafish larvae that might be exploited in screening of chemical libraries to find ameliorative drugs.

Results: We generated clutches of wild type and heterozygous *psen1*^{Q96_K97del} 7 dpf larvae using a paired-mating strategy to reduce extraneous genetic variation before performing a comparative transcriptome analysis. We identified 228 differentially expressed genes and performed various bioinformatics analyses to predict cellular functions.

(Continued on next page)

* Correspondence: michael.lardelli@adelaide.edu.au

¹Alzheimer's Disease Genetics Laboratory, School of Biological Sciences, University of Adelaide, North Terrace, Adelaide, SA 5005, Australia
Full list of author information is available at the end of the article



© The Author(s). 2021 **Open Access** This article is licensed under a Creative Commons Attribution 4.0 International License, which permits use, sharing, adaptation, distribution and reproduction in any medium or format, as long as you give appropriate credit to the original author(s) and the source, provide a link to the Creative Commons licence, and indicate if changes were made. The images or other third party material in this article are included in the article's Creative Commons licence, unless indicated otherwise in a credit line to the material. If material is not included in the article's Creative Commons licence and your intended use is not permitted by statutory regulation or exceeds the permitted use, you will need to obtain permission directly from the copyright holder. To view a copy of this licence, visit <http://creativecommons.org/licenses/by/4.0/>. The Creative Commons Public Domain Dedication waiver (<http://creativecommons.org/publicdomain/zero/1.0/>) applies to the data made available in this article, unless otherwise stated in a credit line to the data.

(Continued from previous page)

Conclusions: Our analyses predicted a significant effect on oxidative phosphorylation, consistent with our earlier observations of predicted effects on ATP synthesis in adult heterozygous *psen1*^{Q96_K97del} brains. The dysregulation of minichromosome maintenance protein complex (MCM) genes strongly contributed to predicted effects on DNA replication and the cell cycle and may explain earlier observations of genome instability due to *PSEN1* mutation. The upregulation of *crystallin* gene expression may be a response to defective activity of mutant Psen1 protein in endolysosomal acidification. Genes related to extracellular matrix (ECM) were downregulated, consistent with previous studies of EOfAD mutant iPSC neurons and postmortem late onset AD brains. Also, changes in expression of genes controlling iron ion transport were observed without identifiable changes in the prevalence of transcripts containing iron responsive elements (IREs) in their 3' untranslated regions (UTRs). These changes may, therefore, predispose to the apparent iron dyshomeostasis previously observed in 6-month-old heterozygous *psen1*^{Q96_K97del} EOfAD-like mutant brains.

Background

Alzheimer's disease (AD) is a progressive neurodegenerative brain disorder that eventually develops into dementia. AD is a serious worldwide health issue and shows a trend of increasing disease incidence [1]. AD may be classified in numerous ways. Late onset, sporadic AD, occurs after 65 years of age and is the most common form, contributing to more than 95% of AD cases [2]. This form of AD is affected by multiple factors, including age, diet, life style, genetic, and environmental factors [3]. Therefore, it has been difficult to model in animals. An early onset, familial form of AD (EOfAD) shows autosomal, dominant inheritance and contributes less than 5% of all AD cases [4]. As both AD forms share similar pathologies [2], many researchers model EOfAD through genetic manipulation of animals to study AD ontology and pathology in general.

Rodent models are the most commonly used in AD research. However, current transgenic rodent models used in EOfAD studies do not reflect closely the disease state of human patients. In 2017, Hargis and Blalock [5] summarized brain transcriptional profiles in human AD, and compared five transgenic mouse models of AD to human AD profiles. All of these mouse models failed to model the most consistent transcriptional signature of human AD, a downregulation of neuronal and mitochondrial genes. Also, the focus of most AD studies is on the pathologies of the advanced disease, such as the accumulation of amyloid- β peptide and tau protein, and on identification of new biomarkers for early diagnosis. However, there is evidence from transcriptome analysis of post-mortem human brains that the brain state during the AD "prodrome" may differ from that of the overt disease. In an analysis of brains from cognitively normal aged control (AC) individuals, individuals displaying mild cognitive impairment (MCI) or individuals with overt AD, an "inversion" of gene differential expression was noted for genes of numerous functional classes with many genes upregulated in MCI compared to AC but downregulated in AD compared to AC [6]. This means

that comparison of genotype-driven brain transcriptome changes in young adult animal models with those changes seen in postmortem human brains may not help in defining those changes that are critical to initiating the progression to AD.

Our laboratory seeks deeper insight into the early molecular states of brains destined to develop AD to explore disease etiology and molecular mechanisms in the hope of finding treatments that might delay or prevent the disease. We have modeled EOfAD-like mutations in the popular vertebrate animal model, the zebrafish. The zebrafish has a fully sequenced and well annotated genome [7], and has the advantages of rapid development with a relatively short generation time. It is easily manipulated genetically and has the capacity to produce large families of siblings which can then be raised together in the same environment to limit the effects of environmental and genetic noise in molecular analyses [8]. Moreover, zebrafish possess orthologs of the human genes mutated in EOfAD. Most recognized EOfAD-causative mutations have been found in the genes *PSEN1*, *PSEN2* and *APP* [9]. (The majority of these mutations, ~63%, occur in the gene *PSEN1* [10].) The zebrafish orthologs of these genes have been identified as *psen1* [11], *psen2* [12], *appa* and *appb* [13]. Therefore, zebrafish have the potential to model EOfAD mutations for the study of the molecular pathological processes of AD. The zebrafish is also a versatile model for drug screening as its tiny larvae can be obtained in large numbers and arrayed into microtitre plates for molecular, developmental, or behavioural analyses [14].

One EOfAD-like mutation we have generated is *psen1*^{Q96_K97del}, a deletion of 6 nucleotides in the zebrafish *psen1* gene. This mutation deletes 2 codons but maintains the open reading frame, leading to structural and hydrophilicity changes in the first luminal loop of the translated protein. Although this mutation is not the exact equivalent of any currently known human EOfAD mutation, there are numerous similar EOfAD mutations that distort the first luminal loop of human *PSEN1* (e.g.

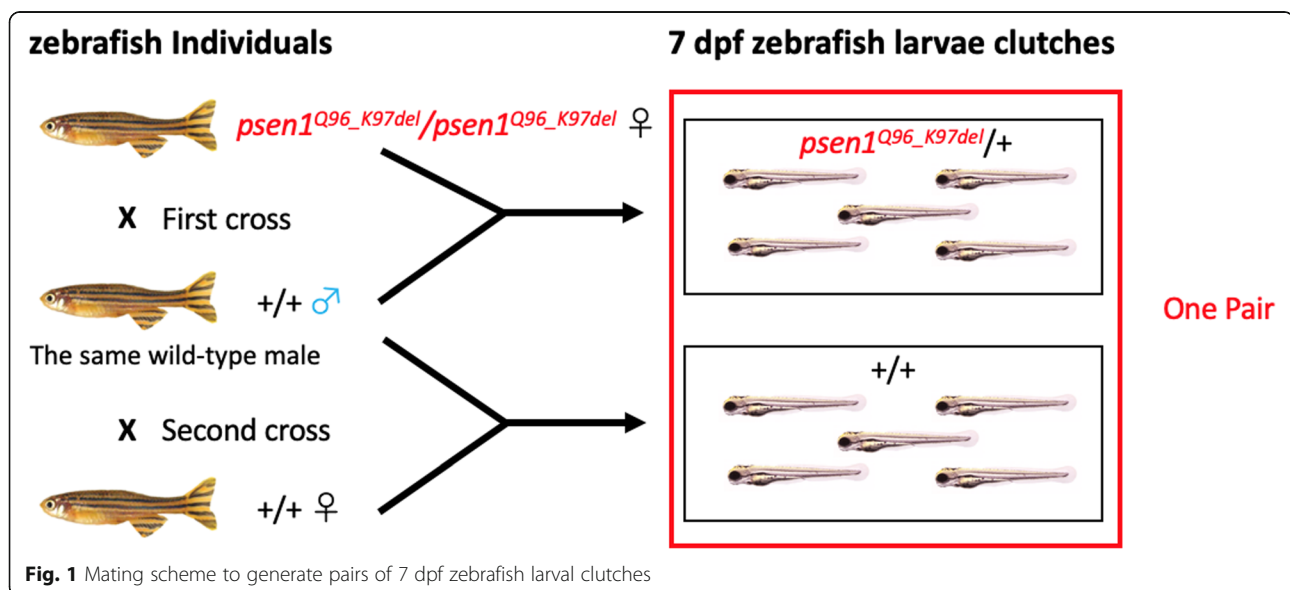
PSEN1^{L113_I114insT} [15], *PSEN1*^{P117L} [16]) and, like all the many various and widely distributed EOfAD mutations in the human *PRESENILIN* genes, it follows the “fAD mutation reading frame preservation rule” [9].

Like human EOfAD mutations, *psen1*^{Q96_K97del} has dominant effects when heterozygous. We have observed that the brains of 6-month-old (young, recently sexually mature adult) zebrafish heterozygous for *psen1*^{Q96_K97del} show transcriptome alterations consistent with disturbances in energy production (ATP synthesis) and lysosomal dysfunction [17]. These may represent the initial stresses that, after decades in humans, lead to AD.

The larvae of zebrafish at 7 days post fertilization (dpf) are only ~ 4 mm in length [18] with a dry mass of ~ 39 µg [19]. They are sufficiently small to be arrayed into 96-well plates for high-throughput screening of chemical libraries to detect potentially therapeutic drugs [20]. Could our heterozygous *psen1*^{Q96_K97del} mutant zebrafish be used to identify drugs that suppress their molecular defects and so might prevent the pathological progression to AD in humans? A 2015 paper by Wagner et al. [21] showed that the most effective drugs in an animal model (of dyslipidemia) were those that best caused reversion of the transcriptomic disease signature to normal. In accordance with this philosophy, we might use our zebrafish mutants to screen for AD-preventative drugs based on the drugs’ ability to revert transcriptomic signatures of ATP synthesis disruption and lysosomal dysfunction back to wild type. Therefore, as a first step in assessing the viability of this idea, we were interested to observe whether the transcriptomic signatures evident in 6-month-old zebrafish *psen1*^{Q96_K97del} heterozygous adult mutant brains were discernable in whole zebrafish larvae.

Our previous analysis of *psen1*^{Q96_K97del} heterozygous adult mutant brain transcriptomes was facilitated by the ability to perform bulk RNA-seq on the entire ~ 7 mg brains of individual mutant zebrafish and their wild type siblings. While an individual zebrafish larva at 7 dpf, (when feeding would normally begin) is too small to provide sufficient RNA for bulk RNA-seq analysis without some form of amplification, we can produce clutches of uniformly heterozygous larvae by crossing a homozygous mutant parent fish with a wild type parent. Analysis of pooled RNA from multiple individuals also reduces between-genotype variability due to “averaging” of the mRNA expression levels contributed by each larva in the pool. Also, using a single male fish to produce both a heterozygous mutant clutch and a wild type clutch of larvae (though mating with a single homozygous mutant or wild type female fish respectively) further reduces genetic variability in the analysis (see Fig. 1).

In this paper we describe a transcriptome analysis on clutches of 7 dpf heterozygous mutant and wild type larvae structured as described above to minimize genetic variation. This identified 228 potentially differentially expressed (DE) genes. Bioinformatic predictive analysis identified probable significant changes in DNA replication and cell cycle processes, to which changes in the regulation of genes related to the minichromosome maintenance protein complex (MCM) were the main contributors. In addition, effects on iron ion transport were identified, suggesting a potential early disruption of iron homeostasis components that might lead, ultimately, to mitochondrial dysfunction including disruption of ATP synthesis.



[26] defined sets of expressed genes that identify different cell types in zebrafish larvae at 5 dpf. Since the cell types present at 5 dpf and 7 dpf do not differ greatly, we used these gene sets to check for changes in expression (implying changes in cell type proportion) between the *psen1*^{Q96_K97del/+} and wild type larvae. The cell types analysed included derivatives of all three germ layers. The analytical procedure followed is described in detail in Supplementary data 1. No significant differences in cell type-specific gene expression were detected, supporting that heterozygosity for the *psen1*^{Q96_K97del} allele does not cause large changes in development.

Differentially expressed genes (DE genes)

Principle component analysis (PCA) was performed and plotted in Fig. 2a, showing that the effects of genotype were captured by PC2 before RUV (removal of unwanted variation, [27]) treatment, while PC1 captured effects of genotype after RUV treatment. Gene expression differences between wild type and heterozygous *psen1*^{Q96_K97del/+} clutches were calculated through a design matrix considering each pair of clutches (see Fig. 1) as a factor and genotypes as the common difference.

Two hundred twenty-eight significantly DE genes were identified (Supplementary data 2) and are highlighted in red on a volcano plot (Fig. 2b). Most of these genes show only minor fold-change differences in expression. Note that, in this analysis, due to the application of RUV, we used a FDR < 0.01 for identification of significantly DE genes, while our previous identification of significantly DE genes in heterozygous mutant 6-month brains did not implement RUV and used a FDR < 0.05 [17]. Comparison of the significantly DE genes identified from heterozygous mutant 7 dpf larvae with those seen in heterozygous mutant 6-month brains [17], revealed only one gene, *lgals8b*, as common between the two datasets. It is upregulated in both.

A variance partitioning analysis was performed to assess the contribution of either “pair” (see Fig. 1) or genotype to the variance in gene expression (Fig. 2c). The contribution of pair to the variance was greater than the contribution of genotype, indicating obvious impacts of parental genetic variation and environmental differences. The contributions of genotype to gene expression variance are listed in the “Genotype” column in Supplementary data 2.

To support the accuracy and reliability of the RNA-seq data, relative standard curve quantitative PCRs (qPCRs) were performed for four of the most statistically significantly DE genes that showed relatively large fold-changes in expression. The qPCRs were performed using cDNA synthesized from the same preparations of RNA that were used in the RNA-seq analysis. Three of the four genes were seen to be differentially expressed to a

statistically significant degree ($p < 0.05$, Supplementary data 3).

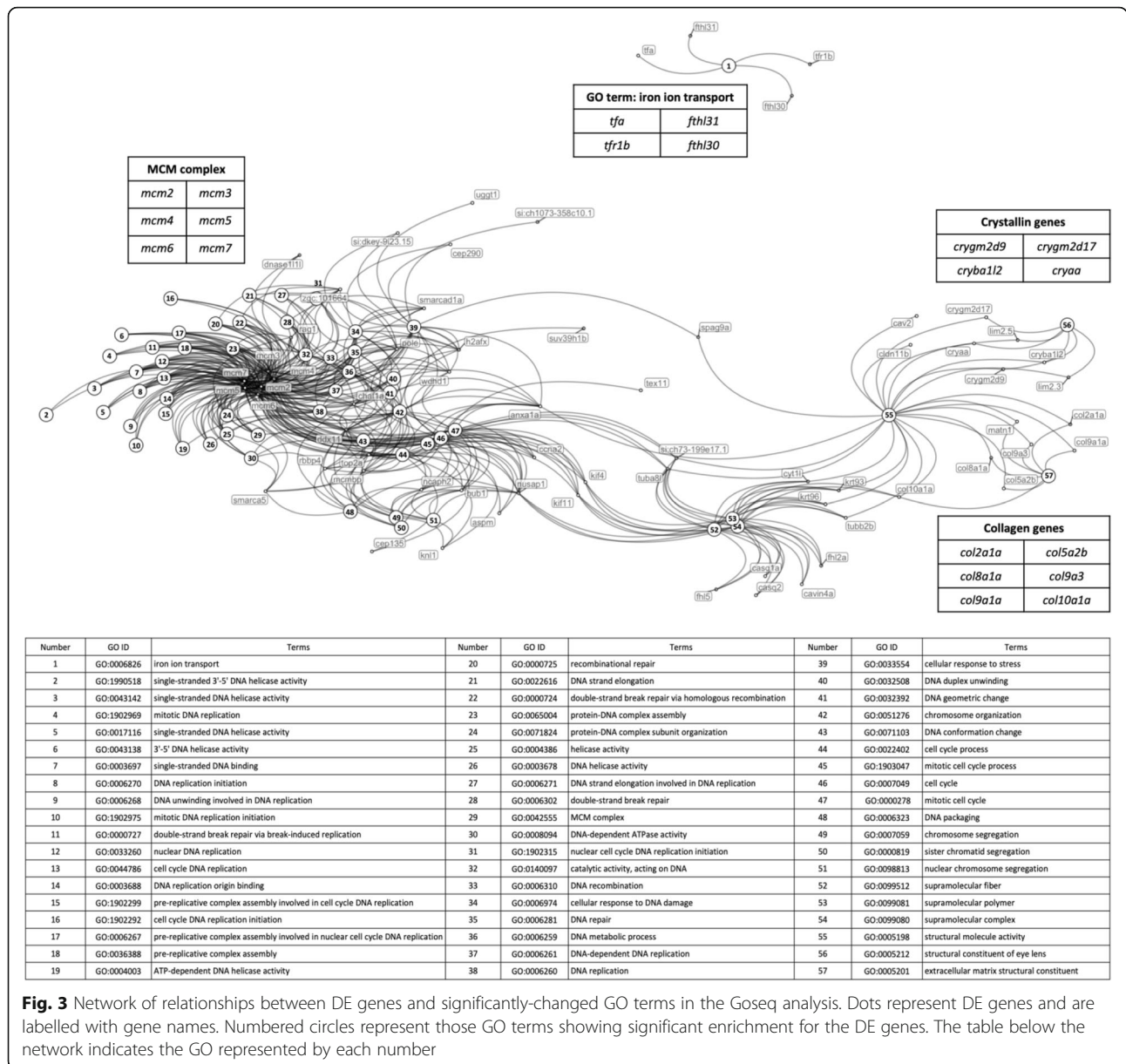
Goseq analysis of pathways and GO terms

To predict the cellular functions affected by heterozygosity for the *psen1*^{Q96_K97del} mutation, we analysed the DE genes using the Hallmark, KEGG, and Wiki pathway databases and the Gene Ontology database. Different pathway databases may contain different representations of similar biological pathways. Hallmark gene sets summarize well-defined biological states or processes built on the overlapping of several gene set collections, and so are useful to achieve an overall view [28]. The KEGG and Wiki gene sets are two popular pathway databases allowing examination of high-level functions. Different pathway databases might show low between-database consistency due to the incomprehensive gene sets and gene interactions in each category [29]. Therefore, to generate a more comprehensive result, we used both KEGG and Wiki pathway databases for pathway analysis.

Pathway and GO analysis were performed using Goseq, which weighted DE genes and calculated each category’s significance amongst DE genes to identify significantly changed pathways or GO terms. Goseq analysis only focuses on the proportions of DE genes in each category but does not consider gene expression fold change and pathway regulation direction. Table 1 shows the Goseq results with a FDR cutoff of 0.05 in the analysis of Hallmark, KEGG and Wiki pathways (Table 1) and of GO terms (Fig. 3). In the Hallmark pathway (Table 1), G2M_CHECKPOINT contains genes critical for cell division cycle progression, and E2F_TARGETS includes numerous genes that play essential roles in the cell cycle and DNA replication [30]. Therefore, the Goseq results of the Hallmark, KEGG and Wiki pathway analyses (Table 1) show significant changes in DNA

Table 1. Significantly-changed pathways in the Goseq analysis of Hallmark, KEGG and Wiki pathways filtered by a FDR cutoff of 0.05

Pathway	DE genes	Genes in category	FDR
<i>Hallmark pathway</i>			
G2M_CHECKPOINT	19	182	1.37E-10
E2F_TARGETS	13	174	2.53E-05
<i>KEGG pathway</i>			
DNA_REPLICATION	7	34	4.17E-06
CELL_CYCLE	8	109	5.29E-04
<i>Wiki pathway</i>			
DNA Replication	6	31	4.26E-05
Cell cycle	7	71	2.08E-04
G1 to S cell cycle control	6	49	2.24E-04



replication and cell cycle control. Among the DE genes in these two categories, most are members of the mini-chromosome maintenance (MCM) protein family. Downregulation of the genes *mcm2*, *mcm3*, *mcm4*, *mcm5*, *mcm6* and *mcm7* were observed in the heterozygous mutant larvae.

In GO analysis, one DE gene can contribute to several related GO terms. The network shown in Fig. 3 illustrates how the DE genes are shared between GO terms. Similar to the pathway analyses, most of the GO terms showing significant enrichment for DE genes are related to the cell cycle and DNA replication. In the network, these GOs cluster around the *MINICHROMOSOME MAINTENANCE (mcm)* genes. The network also

illustrates how numerous genes can form a functionally related cluster contributing to only one or a few GOs. This is seen for the significantly upregulated *CRYSTALLIN* genes that contribute to eye lens structure (GO: *Structural constituent of eye lens*) but also function in lysosomal acidification (not reviewed here, see Discussion). In contrast, the four genes included in the GO *Iron ion transport* show significantly changed regulation. This includes downregulation of the genes *tfa* and *tfr1b* that act to import iron via the endolysosomal pathway [31]. The *ferritin heavy chain like* genes *fthl30* and *fthl31* are upregulated and downregulated respectively, presumably influencing the storage of ferric iron within cells.

We recently published an analysis using a novel method of transcriptome analysis to detect differences in ferrous iron (Fe^{2+}) status in cells [32]. Using this technique, we detected for the first time, that young (6-month-old) adult brains from *psen1*^{Q96_K97del/+} zebrafish are likely deficient for ferrous iron. Therefore, we were very interested to see evidence of iron ion transport gene expression changes in the 7 dpf *psen1*^{Q96_K97del/+} larvae. To confirm the reality of this changed gene expression we performed qPCRs for the genes *tfa*, *tfr1b*, and *fthl31* on cDNA made from the same mRNA samples that were subjected to RNA-seq (see Supplementary data 3, *fthl31* was not examined because its expression level is particularly low). The qPCRs for these three genes were consistent with the RNA-seq results.

When ferrous iron is deficient in cells, Iron Regulatory Proteins bind to Iron-Responsive elements in the 3' untranslated regions (3'UTRs) of mRNAs encoding proteins that function to increase ferrous iron levels (such as human TFR1 [33] or zebrafish *Tfr1b* [34]). To detect ferrous iron dyshomeostasis in transcriptome data, we looked for enrichment of a large set of gene mRNAs that include putative IREs in their 3' UTRs. We did not see enrichment of this gene set in the 7 dpf *psen1*^{Q96_K97del/+} zebrafish larvae, likely indicating that the apparent ferrous iron deficiency of young adult *psen1*^{Q96_K97del/+} brains requires time to develop (Supplementary data 4).

Gene set enrichment analysis (GSEA)

Goseq analysis only focuses on significantly DE genes and predicts affected pathways based on DE gene numbers in each GO. In contrast, GSEA ranks all genes based on fold change and *P*-value, and then estimates their contributions to each pathway. Therefore, GSEA can show pathway regulation direction, and provides a complementary view of gene sets.

We applied GSEA using the Hallmark, KEGG and Wiki pathway databases. Several significantly-changed pathways were identified in each analysis (Table 2), including pathways previously identified in the Goseq pathway analysis. Four of the significantly-changed KEGG pathways are illustrated in Fig. 4. *DNA replication* (Fig. 4a) and *cell cycle* (Fig. 4b) were the most significantly affected pathways identified in the Goseq pathway analysis and the GO analysis. Regulation of the MCM complex plays essential roles in both pathways. The MCM complex forms a DNA helicase, which cooperates with replication protein A (RPA) to unwind duplex parental DNA before DNA synthesis (Fig. 4a, [36]). Dysregulation of the MCM complex would influence DNA replication and might cause replication stress leading to genomic instability [37]. The pathways *ECM receptor interaction* (Fig. 4c) and *oxidative phosphorylation* (OXPHOS, Fig. 4d) were also significantly changed in 7

dpf *psen1*^{Q96_K97del/+} zebrafish larvae. *ECM receptor interaction* was the most significantly changed pathway in KEGG pathway analysis (the lowest *P*-value), and most genes involved were downregulated (Fig. 4c), including the *COLLAGEN* gene group identified in the previous GO analysis. The KEGG pathway *ECM receptor interaction* plays important roles in control of cellular activities, including functioning to provide cell structural support and to regulate cell-cell and cell matrix interactions [38]. In developing brains, *ECM receptor interaction* participates in cell migration and the guidance of growing axons, having crucial effects on neural cells. This has implicated *ECM receptor interaction* in processes underlying many central nervous system (CNS) diseases such as AD, schizophrenia and Parkinson's disease [39]. OXPHOS (Fig. 4d), as well as *fatty acid metabolism* (shown in Table 2), contribute to the fundamentally important function of energy production. In our previous GO analysis of 6-month-old *psen1*^{Q96_K97del/+} zebrafish brains, we saw very significant apparent effects on ATP synthesis [17]. The analysis here suggests that that energy production capacity is downregulated in the mutant larvae and this is expected to include ATP synthesis. Furthermore, *Beta-alanine metabolism*, *glutathione metabolism*, *pyrimidine metabolism*, *butanoate metabolism* and *focal adhesion* are also identified as significantly-changed pathways (Table 2). The interpretation of these pathway changes requires further investigation. KEGG diagrams for the statistically significantly affected pathways not shown in Fig. 4 are given in Supplementary data 5.

We also performed weighted gene co-expression network analysis (WGCNA), but did not identify any informative enriched networks (Supplementary data 6). Normally more than 20 samples should be used in WGCNA, and a minimum recommended sample size is 15 samples [40]. Correlations on fewer than 15 samples are usually too noisy for the identification of biologically meaningful networks. As only 12 samples were used in our transcriptome analysis, our failure to identify informative enriched networks is unsurprising.

Discussion

Heterozygosity for an EOfAD-like mutation of *psen1* has early detectable effects

EOfAD is an adult-onset disease and heterozygosity for EOfAD mutations in human *PSEN1* allows (as far as we know) normal embryo development. However, changes in brain structure and function have been observed by MRI in *PSEN1* EOfAD mutation carrier children as young as 9 years of age [41]. In this study, we observed molecular level (transcriptome) effects of heterozygosity for an EOfAD-like mutation of *psen1* at the very early age of 7 dpf without evidence for changes in cell type

Table 2. Significantly-changed pathways in the GSEA analysis of Hallmark, KEGG and Wiki pathways filtered by a Bonferroni correction P-value of 0.05. ES and NES indicate enrichment score and normalized enrichment score respectively. NES is generated through normalizing enrichment score to mean enrichment score of random samples. Size presents the numbers of genes contributing to each pathway

Pathway	ES	NES	size	padj
Hallmark pathway				
OXIDATIVE_PHOSPHORYLATION	-0.555804281	-1.899952116	202	6.10E-04
MTORC1_SIGNALING	-0.532824812	-1.8177652	198	6.12E-04
XENOBIOTIC_METABOLISM	-0.524048494	-1.783121213	193	6.14E-04
GLYCOLYSIS	-0.534085982	-1.81565734	191	6.15E-04
EPITHELIAL_MESENCHYMAL_TRANSITION	-0.53480945	-1.814489884	187	6.17E-04
G2M_CHECKPOINT	-0.715387358	-2.420487445	182	6.20E-04
E2F_TARGETS	-0.687885552	-2.316955128	174	6.24E-04
FATTY_ACID_METABOLISM	-0.564815428	-1.883230276	157	6.32E-04
CHOLESTEROL_HOMEOSTASIS	-0.655693592	-1.997376931	76	6.96E-04
INTERFERON_GAMMA_RESPONSE	-0.524159178	-1.741314463	152	0.004444049
ESTROGEN_RESPONSE_LATE	-0.478794934	-1.631035008	195	0.009199858
COAGULATION	-0.542963825	-1.750486063	117	0.010511102
MYC_TARGETS_V1	-0.475280378	-1.620439179	197	0.011637736
MYOGENESIS	-0.464741292	-1.580492418	192	0.035661584
KEGG pathway				
ECM_RECEPTOR_INTERACTION	-0.687182381	-2.073168142	71	0.002601799
FATTY_ACID_METABOLISM	-0.753821419	-2.097193508	43	0.002766581
BETA_ALANINE_METABOLISM	-0.834990432	-2.046674914	22	0.002964805
GLUTATHIONE_METABOLISM	-0.729274008	-2.020247611	42	0.005551576
CELL_CYCLE	-0.581949911	-1.860528972	109	0.007407899
DNA_REPLICATION	-0.732012688	-1.95378306	34	0.014165169
PYRIMIDINE_METABOLISM	-0.583500782	-1.816436301	89	0.022831735
BUTANOATE_METABOLISM	-0.741595286	-1.931869094	30	0.025837321
FOCAL_ADHESION	-0.484232114	-1.642520802	186	0.032170787
OXIDATIVE_PHOSPHORYLATION	-0.537913914	-1.751874325	127	0.036339481
WIKI pathway				
Cell cycle	-0.699655808	-2.108960687	71	0.001162888
G1 to S cell cycle control	-0.736907821	-2.097483391	49	0.001214409
DNA Replication	-0.80698873	-2.117293192	31	0.001272343
Cholesterol Biosynthesis	-0.837022118	-1.894160937	15	0.020452081

proportions. This is consistent with the possibility of early changes in brain function. However, the single cell transcriptomic analysis of 5 dpf larvae by Farnsworth et al. observed less than 12% of cells as originating from the CNS [26] so the transcriptome effects of the EOfAD-like *psen1*^{Q96_K97del} mutation that we have observed are likely systemic. Interestingly, peripheral manifestations of Alzheimer's disease have previously been noted (e.g. [42, 43]) and the diverse roles of the Presenilin proteins in cell biology (via their actions in regulating mitochondrial activity [44, 45], in the endolysosomal pathway [46, 47], and in the γ -secretase complex that cleaves at least 149 protein

substrates [48]) are consistent with EOfAD-like mutations having systemic effects outside the CNS. The accessibility of zebrafish embryos and larvae for single cell transcriptome analysis [26], and for real-time observation of neural activity (e.g. [49]) make them excellent tools for future investigation of both the CNS-specific and the systemic actions of *presenilin* mutations.

No suitable transcriptome biomarkers identified for drug screening

Zebrafish larvae represent a powerful system for screening of chemical libraries in drug discovery [14].

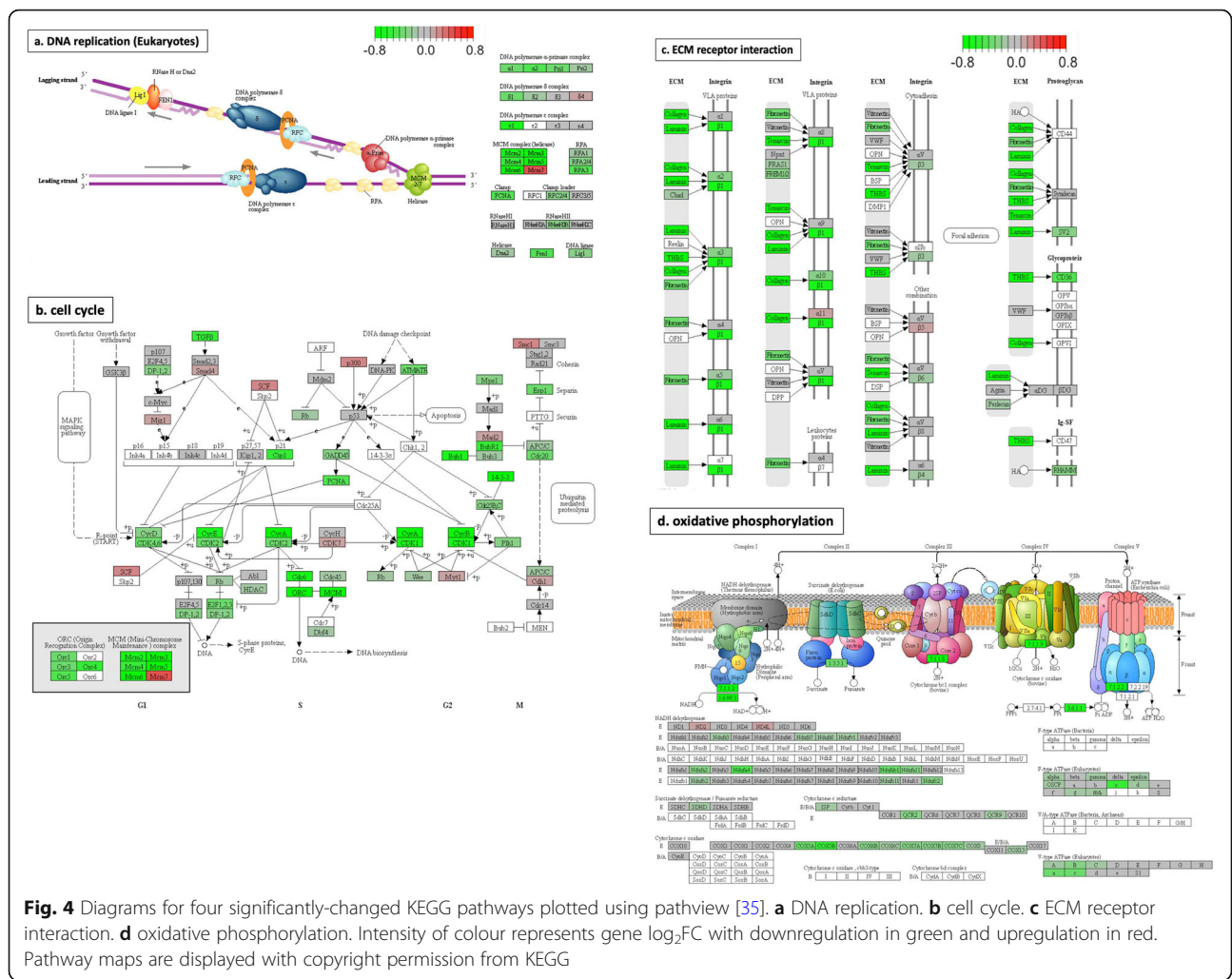


Fig. 4 Diagrams for four significantly-changed KEGG pathways plotted using pathview [35]. **a** DNA replication. **b** cell cycle. **c** ECM receptor interaction. **d** oxidative phosphorylation. Intensity of colour represents gene log₂FC with downregulation in green and upregulation in red. Pathway maps are displayed with copyright permission from KEGG

However, the lack of consistency in transcriptome changes seen between heterozygous mutant *psen1*^{Q96_K97del} 7 dpf larvae compared to heterozygous mutant 6-month-old brains would appear to preclude the use of these mutant larvae to find drugs to suppress the transcriptome changes seen in the brains. While one might consider screening for drugs that suppress the transcriptome changes seen in the larvae (in the hope that these might also have a positive effect on adult brains) the expression levels of the larval DE genes were quite variable between clutches of the same genotype, either wild type or mutant (Supplementary data 3) despite that the RNAs used for the transcriptome analyses were extracted from clutches of larvae rather than individuals. We have also observed high between-sample variability in the expression of individual genes in our previous analyses of zebrafish brains heterozygous for *psen1* mutations [50]. This may be a consequence of the subtlety of the effects produced by such mutations, consistent with the viability and late phenotype onset of disease-related mutations in human *PSEN1* [51, 52].

We were able to identify significantly changed cellular pathways in common between the larvae and adult brains. These related to oxidative phosphorylation, mitochondrial function and lysosomal acidification, indicating that similar stresses/biological effects caused by the presence of the *psen1*^{Q96_K97del} mutation likely exist during the entirety of zebrafish development from larvae to young adult. However, analysis of transcriptomes at this level would be unsuitable for the massively parallel screening of chemical libraries. Therefore, use of the *psen1*^{Q96_K97del} EOFAD-like mutation for discovery of AD-preventative drugs remains infeasible until a suitable biomarker can be identified.

MCM complex dysregulation may drive DNA replication stress
 Comparison of the transcriptomes of pools of 7 dpf heterozygous *psen1*^{Q96_K97del} mutant larvae to their wild type siblings revealed highly significant regulatory effects on genes involved with DNA replication and the cell cycle. These were identified by both Goseq analysis and GSEA. The majority of DE genes contributing to these two terms are related to the minichromosome maintenance

(MCM) protein family. The eukaryotic MCM complex functions as a DNA helicase essential for DNA replication and cell division. The complex is comprised of the protein products of six genes, MCM2–7 (Fig. 4a, [53]). We observed a downregulation of zebrafish genes *mcm2*, *mcm3*, *mcm4*, *mcm5*, *mcm6* and *mcm7* and an upregulation of *mcm7*. If this gene dysregulation phenomenon affects other vertebrates, including mammals, it may clarify a hitherto unexplained mutagenic effect of EOfAD mutations in, specifically, *PSEN1*. In 2002, Chan et al. [54] showed that forced expression of EOfAD mutant *PSEN1*, but not wild type *PSEN1*, increased the sensitivity of Rat pheochromocytoma (PC12) cells to DNA damage by etoposide. Responses included greater than normal increases in p53 protein levels and phosphorylation. In 2010, Michelsen et al. [55], studied the effects in mouse brains of transgenes expressing EOfAD mutant forms of the genes *APP*, or *PSEN1*, or both simultaneously. They observed an increase in the number of single-strand DNA breaks occurring in hippocampal granule cells of the dentate gyrus and hippocampal pyramidal cells in areas CA1/2 when brains expressed only the *PSEN1* mutant transgene. Interestingly, simultaneous expression of EOfAD mutant forms of both *APP* and *PSEN1* reduced the single strand break rate so that it was similar to that seen for only *APP* mutant transgene expression alone. In mice, reduced function of the *Mcm4* gene led to susceptibility to chromosome breaks induced by a DNA replication inhibitor, aphidicolin [56]. Notably, in 2011, Yurov et al. [37] suggested a DNA replication stress hypothesis of AD which proposes that replication stress caused by incomplete DNA replication leads to DNA damage or improper repair, subsequently resulting in the accumulation of genomic instabilities in AD brains. Genomic instabilities are associated with neurodegeneration in other aging-related diseases [57, 58]. Our observations, those of others (above), and Yurov et al.'s ideas suggest that associations between *PSEN1* functions and DNA integrity are an interesting area for further exploration and may give us greater insight into cellular stresses driving AD pathologies.

Are crystallin genes upregulated due to disturbance of lysosomal acidification?

The discovery that DE genes were enriched under the GO term *structural constituent of eye lens*, focused our attention on the crystallin genes *crygm2d9*, *crygm2d17*, *cryba1l2*, and *cryaa*. Crystallin genes have not previously been linked with AD or *PSEN* functions. However, a paper by Valapala et al., 2013 [59] reported that the loss of the β A3/A1-crystallin gene in rat (*Cryba1*) reduces endolysosomal acidification, leading to reduced γ -secretase-mediated release of Notch intracellular domain (NICD) and impaired lysosomal-mediated degradation of Notch. Overexpression of *Cryba1* in a *Cryba1*^{-/-}

knockout mouse apparently was able to rescue the deficient function of the vacuolar ATPase (v-ATPase) responsible for endolysosomal acidification. EOfAD mutations of human *PSEN1* are thought to reduce lysosomal acidification due to a requirement for the PSEN1 holoprotein for correct N-glycosylation of the v-ATPase subunit, V0a1 [46]. Our transcriptome analysis of the effect of heterozygosity for the *psen1*^{Q96_K97del} mutation on 6-month-old zebrafish brains also observed implied effects on lysosomal acidification [17]. While lysosomal acidification was not revealed as an affected GO in our analysis of 7 dpf heterozygous *psen1*^{Q96_K97del} larvae, we speculate that the upregulation of crystallin genes observed may be a homeostatic response to cope with disturbed lysosomal acidification.

Interestingly, Notch signaling has been seen to control expression of the protein products of the human *mcm* gene orthologues, *MCM2* and *MCM6* in cells where Notch signaling suppresses proliferation [60]. However, since Notch signaling was seen to downregulate these proteins, loss of Notch signaling due to increased lysosomal pH would not appear to explain the downregulation of *mcm2* and *mcm6* gene expression we observed in the heterozygous mutant zebrafish larvae.

Does downregulation of ECM-related genes increase the risk of AD?

The most significant KEGG pathway identified in GSEA was *ECM (extracellular matrix) receptor interaction*. Most genes in this pathway, including those encoding collagen, laminin, tenascin and thrombospondin, were significantly downregulated (Fig. 4c). *ECM receptor interaction* is not currently a focus in AD studies, although altered regulation of these genes has previously been observed in some AD relevant research. In 2019, Kwart et al. [61] identified 1515 overlapping DE genes from three human iPSC lines carrying EOfAD mutations in *APP* and *PSEN1*. These DE genes were used to perform an enrichment analysis, and *ECM receptor interaction* was the second most statistically significant KEGG pathway identified. However, the relationships between EOfAD mutations and *ECM receptor interaction* have not been explored further. Another study by Conejero-Goldberg et al., 2014 [62] analysed human postmortem cortex and identified upregulation of ECM-related gene transcripts in carriers of the AD-protective ϵ 2 allele of the gene *APOE* (i.e. APOE2). Based on this observation, they assumed increased ECM expression would reduce amyloid- β secretion or excitotoxicity. Thus, it appears that increased ECM gene expression is associated with decreased AD risk while EOfAD mutation-associated decrease of ECM gene expression promotes AD pathology. This may indicate the potential for ECM gene expression to act as an AD risk

biomarker. More attention should be focused on ECM gene expression in future studies of AD.

Mitochondrial dysfunction is an early effect of the *psen1*^{Q96_K97del} mutation

In addition to the pathways mentioned above, *fatty acid metabolism*, *oxidative phosphorylation (OX PHOS)* and *cholesterol biosynthesis* were identified in the GSEAs of KEGG and Wiki pathways. These pathways represent linked systems that control ATP production to meet cellular energy demand and in response to oxygen availability. Acetyl-CoA, as the starting point of *cholesterol biosynthesis*, is produced by oxidation reactions including oxidative decarboxylation of pyruvate and β -oxidation of fatty acids [63], and is a substrate in the tricarboxylic acid cycle (TCA cycle) to drive oxidative phosphorylation [64]. The AD brain is hypometabolic [65] and mitochondrial dysfunction is associated with oxidative stress in AD neuropathology through reduced ATP production [66]. Reductions in oxidative phosphorylation enzyme activities and functions have been identified in AD and other neurodegenerative processes [67]. A study by Manczak et al. [68] examined the expression of oxidative phosphorylation genes in AD patients and found downregulation of mitochondrial genes coding for electron transport chain (ETC) complex I, which is consistent with the gene expression in our mutant larvae (Fig. 4d). However, Manczak et al. saw increased mRNA expression for components of complexes III and VI in contrast to our observations in mutant larvae. A more recent analysis by Mastroeni et al. [69] saw downregulation of nuclear-encoded ETC genes in AD but increased expression of these relative to age-matched controls in mild cognitive impairment (MCI). The downregulation of *fatty acid metabolism*, *oxidative phosphorylation (OX PHOS)* and *cholesterol biosynthesis* genes observed in mutant larvae indicates that the implied impairment of energy production by the EOfAD-like *psen1*^{Q96_K97del} mutation occurs early in life. Interestingly, decreased expression of genes involved in oxidative phosphorylation was also observed in the brains of zebrafish heterozygous for an EOfAD-like mutation in the gene orthologous to human *SORL1* [70]. This supports that changes in oxidative phosphorylation may be a common “signature” effect of EOfAD mutations in different genes.

Iron homeostasis

We have previously proposed that cellular iron dyshomeostasis may represent a unifying effect-in-common of the EOfAD mutations in *APP*, *PSEN1* and *PSEN2* [31] since *APP* was thought to stabilize the iron export protein FERROPORTIN [71], while endolysosomal acidification (affected by EOfAD mutations in *PSEN1* [46]) is important for import of iron into cells [72]. Recently, the

role of *APP* in stabilization of FERROPORTIN has been challenged [73, 74]. However, it has been revealed that EOfAD mutations in *APP*, (like those in *PSEN1*), also affect acidification of the endolysosomal pathway [75] and so would be expected to affect cellular iron homeostasis. Our identification that the GO *iron ion transport* is affected in 7 dpf *psen1*^{Q96_K97del/+} larvae, particularly with downregulation of the *tfa* and *tfr1b* genes required for importation of iron, supports that EOfAD mutations in *PSEN1* disturb ferrous iron homeostasis. The fact that we have seen transcriptome evidence for such dyshomeostasis in 6-month-old *psen1*^{Q96_K97del/+} brains [17] but were unable to detect stabilization of mRNAs containing IREs in their 3'UTRs in 7 dpf larvae, suggests that any disruption of ferrous iron homeostasis begins subtly. Therefore, we propose that gene dysregulation promoting ferrous iron dyshomeostasis occurs by 7 dpf, but that the iron dyshomeostasis requires time to develop before it becomes apparent as ferrous iron dyshomeostasis in young adult *psen1*^{Q96_K97del/+} brains. Future examination of larval and brain transcriptomes at ages between 7 dpf and 6 months would illuminate when these become significantly enriched for mRNAs containing IREs in their 3'UTRs suggesting the onset of iron dyshomeostasis.

Conclusions

Heterozygosity for the EOfAD-like mutation, *psen1*^{Q96_K97del}, in 7 dpf zebrafish larvae produces marked effects on genes involved in DNA replication, mitochondrial function, extracellular matrix, iron homeostasis and, likely, endolysosomal pathway acidification. While a number of genes were identified as differentially expressed due to the mutation, there was very little overlap between this set of genes and those genes previously identified as differentially expressed in the brains of 6-month-old heterozygous adult fish. Also, the variability in the expression levels of individual genes, even between batches of larvae, means that none of them appear suitable to act as reliable biomarkers of the mutant transcriptome state to allow for screening for chemical compounds that might normalize (alleviate) that state. Our study illustrates the utility of zebrafish for transcriptome analysis of mutant states in vivo, but indicates a difficulty with adaptation of this system to high-throughput screening of chemical libraries when transcriptome state is to be used as a biomarker.

Methods

Ethics

The research described in this paper was carried out under permit S-2017-073 issued to members of the Alzheimer's Disease Genetics Laboratory by the Animal Ethics Committee of the University of Adelaide.

Zebrafish pair-mating breeding strategy

The zebrafish genetic lines used in this study were bred as stocks within the zebrafish facility of the Alzheimer's Disease Genetics Laboratory of the University of Adelaide. Adult fish were returned to their families after mating. A female zebrafish homozygous for the *psen1*^{Q96_K97del} allele was crossed to a male wild-type fish to generate a clutch of heterozygous *psen1*^{Q96_K97del/+} larvae. The same male wild-type fish was then crossed to a female wild-type fish to generate a clutch of wild-type larvae (Fig. 1). The use of the male fish as the common parent in this mating scheme avoids the possibility that maternal effects might obscure transcriptome differences between the larval genotypes [76]. These two clutches of larvae from an individual male wild-type fish were labeled a "pair" (Fig. 1). From previous work analysing the transcriptomes of *psen1*^{Q96_K97del/+} whole zebrafish brains compared to the brains of wild type siblings [17], we found that $n = 6$ would provide a power of ~70% for detection of fold-change > 2 at a false discovery rate (FDR) of 0.05, across the vast majority of expressed transcripts [22]. Therefore, for this analysis involving pooled larvae, we analysed $n = 6$ pairs of larval clutches. Note that no individual adult fish contributed to more than one larval clutch pair.

Sample preparation and RNA purification

Six pairs of larval clutches were generated as described above (12 clutches in total). The parents of 4 pairs of clutches were approximately 5 months old, while the parents of the other two pairs of clutches were approximately 12 months old. The larvae were raised in E3 medium until 7 days post fertilisation, allowing complete larval yolk absorption but not food intake. This was done to minimize the influence of environmental factors on gene expression. As individual larvae are too small to generate sufficient RNA for bulk RNA-seq analysis, 40 larvae were pooled from each clutch (i.e. a total of 480 larvae were consumed in this experiment). Larvae were cooled on ice as anaesthesia before euthanasia/preservation by replacement of their aqueous medium with 400 μ L of Invitrogen RNAlater™ Stabilization Solution (Thermo Fisher Scientific, Waltham, MA, USA) and then kept at 4 °C for 24 h before storage at -80 °C until lysis for total RNA extraction (below).

Total RNA was extracted from pooled larvae using the mirVana™ miRNA isolation Kit (Ambion, Life Technologies, Thermo Fisher Scientific, Waltham, MA, USA). DNase treatment was performed on RNA to remove remaining genomic DNA using the DNA-free™ Kit (Ambion, Life Technologies, Thermo Fisher Scientific, Waltham, MA, USA). Purified total RNA was then delivered to the Genomics Facility at the South Australian Health and Medical Research Institute (SAHMRI,

Adelaide, Australia) for RNA sequencing. Demultiplexed libraries were provided by the sequencing centre at SAHMRI as 75 bp single-end reads, after using polyA amplification. All libraries were sequenced to a minimum depth of 30 million reads, across two NextSeq lanes which were subsequently merged. The data have been deposited in NCBI Gene Expression Omnibus (GEO) database [77] and are accessible through GEO accession number GSE148631.

Transcriptome data treatment and DE gene identification

Reads from each sample were trimmed using Adapter-Removal [78] setting a minimum quality of 30 and a minimum length of 35. Trimmed reads were aligned to the *Danio rerio* genome Ensembl Release 96 (GRCz11) [79] using STAR v2.5.3a [80], and the aligned reads were assigned to each gene using featureCount [81], specifying that only unique alignments which strictly overlapped exonic regions were counted. The 19,396 genes that received more than 1 count per million reads (CPM) in at least 6 samples, were retained for further analysis. The remaining 12,661 genes were discarded as undetectable genes, giving library sizes ranging between 44,498,373 and 52,779,608 reads. A design matrix was specified with an intercept for each pair and with genotype as the common difference. Variance partition analysis was performed using variancePartition [82] with genotype and pair (see Fig. 1) set as random factors. An initial Differential Gene Expression (DE) analysis was then performed using the glmLRT method as implemented in edgeR [83, 84]. The 5000 lowest ranked genes from this analysis (i.e. with the highest p -value) were selected as unchanged negative control genes and passed to RUVg [27], setting $k = 1$. Principal component analysis (PCA) was performed before and after RUV treatment. After RUV treatment, the same design matrix with the addition of the offset term from RUV was used to perform a new DE analysis. A FDR cutoff of 0.01 was then used to identify a gene as differentially expressed (DE), which is highlighted on the volcano plot of Fig. 2b.

Goseq analysis and gene set enrichment analysis (GSEA)

The mappings linking zebrafish genes to Hallmark/KEGG pathways, Wiki pathways and GO terms were achieved by msigdb [28], rWikipathways [85] and org. Dr.eg [86] respectively. To look for enrichment of gene-sets within our defined set of DE genes, a Probability Weighting Function (PWF) was calculated based on the set DE genes using gene lengths as the bias data. Then goseq analysis [87] was performed using this PWF and gene-sets were considered as significantly enriched in the set of DE genes using a FDR threshold of 0.05.

In order to look at the more complete list of all expressed genes, we then used Gene Set Enrichment

Analysis (GSEA, [88]) as implemented in the *fgsea* [89] package. A ranked list was formed using $\text{sign}(\log_2\text{FC}) * (-\log_{10}\text{PValue})$ as the ranking statistic and the same gene-sets as for *goseq* were tested, using $n = 10^5$ iterations. A Bonferroni corrected p -value < 0.05 was used to identify significantly-altered pathways. Pathway Diagrams for detected KEGG pathways were plotted by *pathview* [35] using $\log_2\text{FC}$.

Iron responsive elements (IRE) enrichment analysis

Genes containing iron responsive elements (IREs) in either the 5' or 3' UTRs of their transcripts were identified using searching for IREs (SIREs) [32, 90]. Both *goseq* [87] and GSEA were performed to detect the enrichments of the genes containing IREs in their 5'UTR or 3'UTR respectively. A FDR and a Bonferroni corrected p -value < 0.05 were used to identify significant enrichments in *goseq* analysis and GSEA respectively.

Abbreviations

AD: Alzheimer's disease; ATP: Adenosine triphosphate; CNS: Central nervous system; CPM: Count(s) per million reads; DE: Differentially expressed; Dpf: Day post fertilization; ECM: Extracellular matrix; EOFAD: Early-onset familial Alzheimer's disease; ETC: Electron transport chain; FC: Fold change; FDR: False discovery rate; GO: Gene Ontology; GSEA: Gene set enrichment analysis; iPSC: Induced pluripotent stem cell; IRE: Iron responsive elements; KEGG: Kyoto Encyclopedia of Genes and Genomes; MCI: Mild cognitive impairment; MCM: Minichromosome maintenance protein complex; NICD: Notch intracellular domain; OX PHOS: Oxidative phosphorylation; PC: Principle component; PCA: Principle component analysis; PWF: Probability Weighting Function; qPCRs: Quantitative PCRs; RUV: Remove unwanted variation (method); SIREs: Searching for IREs (web server); UTRs: Untranslated regions; v-ATPase: Vacuolar ATPase; WGCNA: Weighted gene co-expression network analysis

Supplementary Information

The online version contains supplementary material available at <https://doi.org/10.1186/s12864-021-07509-1>.

Additional file 1: Supplementary data 1. Testing for differences in cell type proportions between genotypes.

Additional file 2: Supplementary data 2. DE genes. A spreadsheet of genes detected as differentially expressed (DE) including information on fold change, p -value, FDR, Rank statistics (for GSEA), and "Genotype" (giving the contribution of genotype to gene expression variance as determined by variance partitioning analysis).

Additional file 3: Supplementary data 3. qPCR validation of RNA-seq data. This file includes information on quantitative PCR (qPCR) method, oligonucleotide PCR primers, and comparison of RNA-seq with qPCR data for a number of genes.

Additional file 4: Supplementary data 4. IRE enrichment analysis. Results from analysis of the enrichment of Iron Responsive Element (IRE) gene sets in the transcriptome data.

Additional file 5: Supplementary data 5. KEGG pathway diagrams. Diagrams for 6 significantly changed KEGG pathways not shown in the main manuscript.

Additional file 6: Supplementary data 6. Weighted gene co-expression network analysis (WGCNA).

Acknowledgements

The authors wish to thank Lachlan Warren William Baer for his technical assistance in construction of the GO plot. We thank the Kyoto Encyclopedia

of Genes and Genomes (KEGG) for copyright permission to display their Pathway Maps.

Authors' contributions

YD and ML conceived the project. MN produced the homozygous parental *psen1^{Q96_K97del}* fish. YD conducted fish mating and collection of larvae, RNA purification and qPCR validation of RNA-seq data. YD performed analysis of RNA-seq data under the guidance of SP except that KB performed the analysis of cell type proportions and NH performed the IRE enrichment analysis. YD drafted the manuscript that was subsequently edited by SP and ML. All authors read and approved the final manuscript.

Funding

YD was supported by an Adelaide Graduate Research Scholarship from the University of Adelaide. ML and MN were both supported by grants GNT1061006 and GNT1126422 from the National Health and Medical Research Council of Australia, <https://www.nhmrc.gov.au/>. ML is supported by a grant from the Carthew Family Charity Trust. ML and SP are employees of the University of Adelaide. NH was supported by an Australian Government Research Training Program (RTP) Scholarship. No funding body played any role in the study design, data collection and analysis, decision to publish, or preparation of the manuscript.

Availability of data and materials

The raw fastq files and the output of *featureCounts* have been deposited in the NCBI Gene Expression Omnibus (GEO) database and are accessible through GEO accession number GSE148631. All data generated or analysed during this study are included in this published article and its supplementary information files, and are accessible through the GitHub repository: https://github.com/yangdongau/20190717_Lardelli_RNASeq_Larvae. Trimmed RNA-seq reads were aligned to the *Danio rerio* genome Ensembl Release 96 (GRCz11) of the Ensembl Project, [79] (www.ensembl.org). Gene Ontology gene sets were obtained from geneontology.org using the *org.Dr.eleg.db* R Package [91]. Hallmark [92] and KEGG [93] gene sets were obtained from the Molecular Signatures Database, MSigDB (<http://www.gsea-msigdb.org/gsea/msigdb/collections.jsp>), using the *msigdb* package [94]. KEGG pathway maps were obtained from KEGG, (<https://www.kegg.jp/>) using the *pathview* R package [35]. Wiki pathway gene sets were obtained from WikiPathways (<https://wikipathways.org>) using the *rWikipathways* R package [85]. Gene sets describing genes expressed within various cell types/tissues in 5 dpf zebrafish larvae were obtained from Table S2 of Farnsworth et al. [26] (<https://www.sciencedirect.com/science/article/pii/S0012160619304919>). Iron Responsive Element (IRE) gene sets are provided in Supplementary Table 1 of Hin et al. [32] (<https://www.biorxiv.org/content/10.1101/2020.05.01.071498v3.supplementary-material>).

Declarations

Ethics approval and consent to participate

The research described in this paper was carried out under permit S-2017-073 from the Animal Ethics Committee of the University of Adelaide.

Consent for publication

Not applicable.

Competing interests

The authors declare that they have no competing interests.

Author details

¹Alzheimer's Disease Genetics Laboratory, School of Biological Sciences, University of Adelaide, North Terrace, Adelaide, SA 5005, Australia. ²Bioinformatics Hub, School of Biological Sciences, University of Adelaide, North Terrace, Adelaide, SA 5005, Australia.

Received: 2 June 2020 Accepted: 5 March 2021

Published online: 24 March 2021

References

- Gaugler J, et al. 2019 Alzheimer's disease facts and figures. *Alzheimers Dement.* 2019;15(3):321–87.

2. Masters CL, Bateman R, Blennow K, Rowe CC, Sperling RA, Cummings JL. Alzheimer's disease. *Nat Rev Dis Primers*. 2015;1(1):15056. <https://doi.org/10.1038/nrdp.2015.56>.
3. Beydoun MA, Beydoun HA, Gamaldo AA, Teel A, Zonderman AB, Wang Y. Epidemiologic studies of modifiable factors associated with cognition and dementia: systematic review and meta-analysis. *BMC Public Health*. 2014;14(1):643. <https://doi.org/10.1186/1471-2458-14-643>.
4. Barber RC. The genetics of Alzheimer's disease. *Scientifica*. 2012;2012:246210.
5. Hargis KE, Blalock EM. Transcriptional signatures of brain aging and Alzheimer's disease: what are our rodent models telling us? *Behav Brain Res*. 2017;322(Pt B):311–28.
6. Berchtold NC, Sabbagh MN, Beach TG, Kim RC, Cribbs DH, Cotman CW. Brain gene expression patterns differentiate mild cognitive impairment from normal aged and Alzheimer's disease. *Neurobiol Aging*. 2014;35(9):1961–72. <https://doi.org/10.1016/j.neurobiolaging.2014.03.031>.
7. Howe K, Clark MD, Torroja CF, Torrance J, Berthelot C, Muffato M, Collins JE, Humphray S, McLaren K, Matthews L, McLaren S, Sealy I, Caccamo M, Churche C, Scott C, Barrett JC, Koch R, Rauch GJ, White S, Chow W, Kilian B, Quintais LT, Guerra-Assunção JA, Zhou Y, Gu Y, Yen J, Vogel JH, Eyre T, Redmond S, Banerjee R, Chi J, Fu B, Langley E, Maguire SF, Laird GK, Lloyd D, Kenyon E, Donaldson S, Sehra H, Almeida-King J, Loveland J, Trevanion S, Jones M, Quail M, Willey D, Hunt A, Burton J, Sims S, McLay K, Plumb B, Davis J, Clew C, Oliver K, Clark R, Riddle C, Elliott D, Threadgold G, Harden G, Ware D, Begum S, Mortimore B, Kerry G, Heath P, Phillimore B, Tracey A, Corby N, Dunn M, Johnson C, Wood J, Clark S, Pelan S, Griffiths G, Smith M, Glithero R, Howden P, Barker N, Lloyd C, Stevens C, Harley J, Holt K, Panagiotidis G, Lovell J, Beasley H, Henderson C, Gordon D, Auger K, Wright D, Collins J, Raisen C, Dyer L, Leung K, Robertson L, Ambridge K, Leongamornlert D, McGuire S, Gilderthorp R, Griffiths C, Manthravadi D, Nichol S, Barker G, Whitehead S, Kay M, Brown J, Murmane C, Gray E, Humphries M, Sycamore N, Barker D, Saunders D, Wallis J, Babbage A, Hammond S, Mashreghi-Mohammadi M, Barr L, Martin S, Wray P, Ellington A, Matthews N, Ellwood M, Woodmansey R, Clark G, Cooper JD, Tromans A, Grafham D, Skuce C, Pandian R, Andrews R, Harrison E, Kimberley A, Garnett J, Fosker N, Hall R, Garner P, Kelly D, Bird C, Palmer S, Gehring I, Berger A, Dooley CM, Ersan-Ürün Z, Eser C, Geiger H, Geisler M, Karotki L, Kirn A, Konantz J, Konantz M, Oberländer M, Rudolph-Geiger S, Teucke M, Lanz C, Raddatz G, Osoegawa K, Zhu B, Rapp A, Widaa S, Langford C, Yang F, Schuster SC, Carter NP, Harrow J, Ning Z, Herrero J, Searle SMJ, Enright A, Geisler R, Plasterk RHA, Lee C, Westerfield M, de Jong PJ, Zon LI, Postlethwait JH, Nüsslein-Volhard C, Hubbard TJP, Crollius HR, Rogers J, Stemple DL. The zebrafish reference genome sequence and its relationship to the human genome. *Nature*. 2013;496(7446):498–503. <https://doi.org/10.1038/nature12111>.
8. Newman M, Ebrahimie E, Lardelli M. Using the zebrafish model for Alzheimer's disease research. *Front Genet*. 2014;5:189.
9. Jayne T, Newman M, Verdile G, Sutherland G, Münch G, Musgrave I, Moussavi Nik SH, Lardelli M. Evidence for and against a pathogenic role of reduced gamma-Secretase activity in familial Alzheimer's disease. *J Alzheimers Dis*. 2016;52(3):781–99. <https://doi.org/10.3233/JAD-151186>.
10. Pottier C, et al. High frequency of potentially pathogenic SORL1 mutations in autosomal dominant early-onset Alzheimer disease. *Mol Psychiatry*. 2012;17(9):875–9. <https://doi.org/10.1038/mp.2012.15>.
11. Leimer U, Lun K, Romig H, Walter J, Grünberg J, Brand M, Haass C. Zebrafish (*Danio rerio*) presenilin promotes aberrant amyloid beta-peptide production and requires a critical aspartate residue for its function in amyloidogenesis. *Biochemistry*. 1999;38(41):13602–9. <https://doi.org/10.1021/bi991453n>.
12. Groth C, Nornes S, McCarty R, Tamme R, Lardelli M. Identification of a second presenilin gene in zebrafish with similarity to the human Alzheimer's disease gene presenilin2. *Dev Genes Evol*. 2002;212(10):486–90. <https://doi.org/10.1007/s00427-002-0269-5>.
13. Musa A, Lehrach H, Russo VA. Distinct expression patterns of two zebrafish homologues of the human APP gene during embryonic development. *Dev Genes Evol*. 2001;211(11):563–7. <https://doi.org/10.1007/s00427-001-0189-9>.
14. Parg C, Seng WL, Semino C, McGrath P. Zebrafish: a preclinical model for drug screening. *Assay Drug Dev Technol*. 2002;1(1):41–8. <https://doi.org/10.1089/15406580271601293>.
15. De Jonghe C, et al. Aberrant splicing in the presenilin-1 intron 4 mutation causes presenile Alzheimer's disease by increased Abeta42 secretion. *Hum Mol Genet*. 1999;8(8):1529–40. <https://doi.org/10.1093/hmg/8.8.1529>.
16. Wisniewski T, Dowjat WK, Buxbaum JD, Khorkova O, Efthimiopoulos S, Kulczycki J, Lojkowska W, Wegiel J, Wisniewski HM, Frangione B. A novel polish presenilin-1 mutation (P117L) is associated with familial Alzheimer's disease and leads to death as early as the age of 28 years. *Neuroreport*. 1998;9(2):217–21. <https://doi.org/10.1097/00001756-199801260-00008>.
17. Newman M, Hin N, Pederson S, Lardelli M. Brain transcriptome analysis of a familial Alzheimer's disease-like mutation in the zebrafish presenilin 1 gene implies effects on energy production. *Mol Brain*. 2019;12(1):43. <https://doi.org/10.1186/s13041-019-0467-y>.
18. Parichy DM, Elizondo MR, Mills MG, Gordon TN, Engeszer RE. Normal table of postembryonic zebrafish development: staging by externally visible anatomy of the living fish. *Dev Dyn*. 2009;238(12):2975–3015. <https://doi.org/10.1002/dvdy.22113>.
19. Petersen GI, Kristensen P. Bioaccumulation of lipophilic substances in fish early life stages. *Environ Toxicol Chem*. 1998;17(7):1385–95. <https://doi.org/10.1002/etc.5620170724>.
20. Richter S, Schulze U, Tomançak P, Oates AC. Small molecule screen in embryonic zebrafish using modular variations to target segmentation. *Nat Commun*. 2017;8(1):1901. <https://doi.org/10.1038/s41467-017-01469-5>.
21. Wagner A, Cohen N, Kelder T, Amit U, Liebman E, Steinberg DM, Radonjic M, Ruppel E. Drugs that reverse disease transcriptomic signatures are more effective in a mouse model of dyslipidemia. *Mol Syst Biol*. 2015;11(3):791. <https://doi.org/10.15252/msb.20145486>.
22. Zhao S, Li CI, Guo Y, Sheng Q, Shyr Y. RnaSeqSampleSize: real data based sample size estimation for RNA sequencing. *BMC Bioinformatics*. 2018;19(1):191. <https://doi.org/10.1186/s12859-018-2191-5>.
23. Papadopoulou AA, Fluhrer R. Signaling functions of intramembrane Aspartyl-proteases. *Front Cardiovasc Med*. 2020;7:591787. <https://doi.org/10.3389/fcvm.2020.591787>.
24. Gowrishankar K, Zeidler MG, Vincenz C. Release of a membrane-bound death domain by gamma-secretase processing of the p75NTR homolog NRADD. *J Cell Sci*. 2004;117(Pt 18):4099–111. <https://doi.org/10.1242/jcs.01263>.
25. Krishnamurthy N, Kurzrock R. Targeting the Wnt/beta-catenin pathway in cancer: update on effectors and inhibitors. *Cancer Treat Rev*. 2018;62:50–60. <https://doi.org/10.1016/j.ctrv.2017.11.002>.
26. Farnsworth DR, Saunders LM, Miller AC. A single-cell transcriptome atlas for zebrafish development. *Dev Biol*. 2020;459(2):100–8. <https://doi.org/10.1016/j.ydbio.2019.11.008>.
27. Riso D, Ngai J, Speed TP, Dudoit S. Normalization of RNA-seq data using factor analysis of control genes or samples. *Nat Biotechnol*. 2014;32(9):896–902. <https://doi.org/10.1038/nbt.2931>.
28. Liberzon A, Birger C, Thorvaldsdóttir H, Ghandi M, Mesirov JP, Tamayo P. The molecular signatures database Hallmark gene set collection. *Cell Syst*. 2015;1(6):417–25. <https://doi.org/10.1016/j.cels.2015.12.004>.
29. Soh D, Dong D, Guo Y, Wong L. Consistency, comprehensiveness, and compatibility of pathway databases. *BMC Bioinformatics*. 2010;11(1):449. <https://doi.org/10.1186/1471-2105-11-449>.
30. Bracken AP, Ciro M, Cocito A, Helin K. E2F target genes: unraveling the biology. *Trends Biochem Sci*. 2004;29(8):409–17. <https://doi.org/10.1016/j.tibs.2004.06.006>.
31. Lumsden AL, Rogers JT, Majd S, Newman M, Sutherland GT, Verdile G, Lardelli M. Dysregulation of neuronal iron homeostasis as an alternative unifying effect of mutations causing familial Alzheimer's disease. *Front Neurosci*. 2018;12:533. <https://doi.org/10.3389/fnins.2018.00533>.
32. Hin, N, et al. Iron Responsive Element (IRE)-mediated responses to iron dyshomeostasis in Alzheimer's disease. *bioRxiv*, 2020: p. 2020.05.01.071498.
33. Anderson GJ, Frazer DM. Current understanding of iron homeostasis. *Am J Clin Nutr*. 2017;106(Suppl 6):1559S–66S. <https://doi.org/10.3945/ajcn.117.155804>.
34. Ye H, Rouault TA. Erythropoiesis and iron sulfur cluster biogenesis. *Adv Hematol*. 2010;2010:1–8. <https://doi.org/10.1155/2010/329394>.
35. Luo W, Brouwer C. Pathview: an R/bioconductor package for pathway-based data integration and visualization. *Bioinformatics*. 2013;29(14):1830–1. <https://doi.org/10.1093/bioinformatics/btt285>.
36. Waga S, Stillman B. The DNA replication fork in eukaryotic cells. *Annu Rev Biochem*. 1998;67(1):721–51. <https://doi.org/10.1146/annurev.biochem.67.1.721>.
37. Yurov YB, Vorsanova SG, Lourov IY. The DNA replication stress hypothesis of Alzheimer's disease. *Sci World J*. 2011;11:2602–12. <https://doi.org/10.1100/2011/625690>.
38. Van der Ven AT, Vivante A, Hildebrandt F. Novel insights into the pathogenesis of monogenic congenital anomalies of the kidney and urinary tract. *J Am Soc Nephrol*. 2018;29(1):36–50. <https://doi.org/10.1681/ASN.2017050561>.

39. Berezin V, et al. Targeting of ECM molecules and their metabolizing enzymes and receptors for the treatment of CNS diseases. *Prog Brain Res*. 2014;214:353–88. <https://doi.org/10.1016/B978-0-444-63486-3.00015-3>.
40. Langfelder P, Horvath S. WGCNA: an R package for weighted correlation network analysis. *BMC Bioinformatics*. 2008;9(1):559. <https://doi.org/10.1186/1471-2105-9-559>.
41. Quiroz YT, Schultz AP, Chen K, Protas HD, Brickhouse M, Fleisher AS, Langbaum JB, Thiyagura P, Fagan AM, Shah AR, Muniz M, Arboleda-Velasquez JF, Munoz C, Garcia G, Acosta-Baena N, Giraldo M, Tirado V, Ramirez DL, Tariot PN, Dickerson BC, Sperling RA, Lopera F, Reiman EM. Brain imaging and blood biomarker abnormalities in children with autosomal dominant Alzheimer disease: a cross-sectional study. *JAMA Neurol*. 2015;72(8):912–9. <https://doi.org/10.1001/jamaneurol.2015.1099>.
42. Tublin JM, Adelstein JM, del Monte F, Combs CK, Wold LE. Getting to the heart of Alzheimer disease. *Circ Res*. 2019;124(1):142–9. <https://doi.org/10.1161/CIRCRESAHA.118.313563>.
43. Morris JK, Honea RA, Vidoni ED, Swerdlow RH, Burns JM. Is Alzheimer's disease a systemic disease? *Biochim Biophys Acta (BBA) - Mol Basis Dis*. 2014;1842(9):1340–9. <https://doi.org/10.1016/j.bbadis.2014.04.012>.
44. Area-Gomez E, de Groof A, Bonilla E, Montesinos J, Tanji K, Boldogh I, Pon L, Schon EA. A key role for MAM in mediating mitochondrial dysfunction in Alzheimer disease. *Cell Death Dis*. 2018;9(3):335. <https://doi.org/10.1038/s41419-017-0215-0>.
45. Pera M, Larrea D, Guardia-Laguarta C, Montesinos J, Velasco KR, Agrawal RR, Xu Y, Chan RB, di Paolo G, Mehler MF, Perumal GS, Macaluso FP, Freyberg ZZ, Acin-Perez R, Enriquez JA, Schon EA, Area-Gomez E. Increased localization of APP-C99 in mitochondria-associated ER membranes causes mitochondrial dysfunction in Alzheimer disease. *EMBO J*. 2017;36(22):3356–71. <https://doi.org/10.15252/embj.201796797>.
46. Lee JH, Yu WH, Kumar A, Lee S, Mohan PS, Peterhoff CM, Wolfe DM, Martinez-Vicente M, Massey AC, Sovak G, Uchiyama Y, Westaway D, Cuervo AM, Nixon RA. Lysosomal proteolysis and autophagy require presenilin 1 and are disrupted by Alzheimer-related PS1 mutations. *Cell*. 2010;141(7):1146–58. <https://doi.org/10.1016/j.cell.2010.05.008>.
47. Lee JH, McBrayer MK, Wolfe DM, Haslett LJ, Kumar A, Sato Y, Lie P, Mohan P, Coffey EE, Kompella U, Mitchell CH, Lloyd-Evans E, Nixon RA. Presenilin 1 maintains Lysosomal Ca²⁺ homeostasis via TRPML1 by regulating vATPase-mediated lysosome acidification. *Cell Rep*. 2015;12(9):1430–44. <https://doi.org/10.1016/j.celrep.2015.07.050>.
48. Guner G, Lichtenthaler SF. The substrate repertoire of gamma-secretase/presenilin. *Semin Cell Dev Biol*. 2020;105:27–42. <https://doi.org/10.1016/j.semcdb.2020.05.019>.
49. Constantini L, Poulsen RE, Scholz LA, Favre-Bulle IA, Taylor MA, Sun B, Goodhill GJ, Vanwalleghem GC, Scott EK. Altered brain-wide auditory networks in a zebrafish model of fragile X syndrome. *BMC Biol*. 2020;18(1):125. <https://doi.org/10.1186/s12915-020-00857-6>.
50. Dong Y. Investigating Alzheimer's disease using zebrafish genetic models, in school of biological sciences. Adelaide: The University of Adelaide; 2020.
51. Ryman DC, Acosta-Baena N, Aisen PS, Bird T, Danek A, Fox NC, Goate A, Frommelt P, Ghetti B, Langbaum JBS, Lopera F, Martins R, Masters CL, Mayeux RP, McDade E, Moreno S, Reiman EM, Ringman JM, Salloway S, Schofield PR, Sperling R, Tariot PN, Xiong C, Morris JC, Bateman RJ, and the Dominantly Inherited Alzheimer Network. Symptom onset in autosomal dominant Alzheimer disease: a systematic review and meta-analysis. *Neurology*. 2014;83(3):253–60. <https://doi.org/10.1212/WNL.0000000000000596>.
52. Wang B, Yang W, Wen W, Sun J, Su B, Liu B, Ma D, Lv D, Wen Y, Qu T, Chen M, Sun M, Shen Y, Zhang X. Gamma-secretase gene mutations in familial acie inversa. *Science*. 2010;330(6007):1065. <https://doi.org/10.1126/science.1196284>.
53. Li N, Zhai Y, Zhang Y, Li W, Yang M, Lei J, Tye BK, Gao N. Structure of the eukaryotic MCM complex at 3.8 Å. *Nature*. 2015;524(7564):186–91. <https://doi.org/10.1038/nature14685>.
54. Chan SL, Culmsee C, Haughey N, Klapper W, Mattson MP. Presenilin-1 mutations sensitize neurons to DNA damage-induced death by a mechanism involving perturbed calcium homeostasis and activation of calpains and caspase-12. *Neurobiol Dis*. 2002;11(1):2–19. <https://doi.org/10.1006/mbdi.2002.0542>.
55. Michelsen KA, Korr H, Steinbusch HWM, Schmitz C. Presenilin 1-related alterations in DNA integrity in a transgenic mouse model of Alzheimer's disease. *Brain Res*. 2010;1316:139–44. <https://doi.org/10.1016/j.brainres.2009.12.033>.
56. Shima N, Alcaraz A, Liachko I, Buske TR, Andrews CA, Munroe RJ, Hartford SA, Tye BK, Schimenti JC. A viable allele of Mcm4 causes chromosome instability and mammary adenocarcinomas in mice. *Nat Genet*. 2007;39(1):93–8. <https://doi.org/10.1038/ng1936>.
57. Iourov IY, Vorsanova SG, Liehr T, Kolotii AD, Yurov YB. Increased chromosome instability dramatically disrupts neural genome integrity and mediates cerebellar degeneration in the ataxia-telangiectasia brain. *Hum Mol Genet*. 2009;18(14):2656–69. <https://doi.org/10.1093/hmg/ddp207>.
58. Nussenzweig A. Causes and consequences of the DNA damage response. *Cell Cycle*. 2007;6(19):2339–40. <https://doi.org/10.4161/cc.6.19.4995>.
59. Valapala M, Hose S, Gongora C, Dong L, Wawrousek EF, Samuel Zigler J Jr, Sinha D. Impaired endolysosomal function disrupts Notch signalling in optic nerve astrocytes. *Nat Commun*. 2013;4(1):1629. <https://doi.org/10.1038/ncomms2624>.
60. Noseda M, Niessen K, McLean G, Chang L, Karsan A. Notch-dependent cell cycle arrest is associated with downregulation of minichromosome maintenance proteins. *Circ Res*. 2005;97(2):102–4. <https://doi.org/10.1161/01.RES.0000174380.06673.81>.
61. Kwart D, Gregg A, Scheckel C, Murphy EA, Paquet D, Duffield M, Fak J, Olsen O, Darnell RB, Tessier-Lavigne M. A large panel of isogenic APP and PSEN1 mutant human iPSC neurons reveals shared endosomal abnormalities mediated by APP beta-CTFs, Not Abeta. *Neuron*. 2019;104(5):1022. <https://doi.org/10.1016/j.neuron.2019.11.010>.
62. Conejero-Goldberg C, Gomar JJ, Bobes-Bascaran T, Hyde TM, Kleinman JE, Herman MM, Chen S, Davies P, Goldberg TE. APOE2 enhances neuroprotection against Alzheimer's disease through multiple molecular mechanisms. *Mol Psychiatry*. 2014;19(11):1243–50. <https://doi.org/10.1038/mp.2013.194>.
63. Bhagavan NV, Ha CE. Lipids I: fatty acids and eicosanoids, in essentials of medical biochemistry. 2nd ed: Academic Press; 2015. p. 269–97.
64. Martinez-Reyes I, Chandel NS. Mitochondrial TCA cycle metabolites control physiology and disease. *Nat Commun*. 2020;11(1):102. <https://doi.org/10.1038/s41467-019-13668-3>.
65. Mosconi L, Puppi A, De Leon MJ. Brain glucose hypometabolism and oxidative stress in preclinical Alzheimer's disease. *Mitochondrial Oxid Stress Neurodegenerative Disord*. 2008;1147:180–95.
66. Zhang C, Rissman RA, Feng J. Characterization of ATP alternations in an Alzheimer's disease transgenic mouse model. *J Alzheimers Dis*. 2015;44(2):375–8. <https://doi.org/10.3233/JAD-141890>.
67. Shoffner JM. Oxidative phosphorylation defects and Alzheimer's disease. *Neurogenetics*. 1997;1(1):13–9. <https://doi.org/10.1007/s100480050002>.
68. Manczak M, Park BS, Jung Y, Reddy PH. Differential expression of oxidative phosphorylation genes in patients with Alzheimer's disease: implications for early mitochondrial dysfunction and oxidative damage. *NeuroMolecular Med*. 2004;5(2):147–62. <https://doi.org/10.1385/NMM:5:2:147>.
69. Mastroni D, Khodour OM, Delvaux E, Nolz J, Olsen G, Berchtold N, Cotman C, Hecht SM, Coleman PD. Nuclear but not mitochondrial-encoded oxidative phosphorylation genes are altered in aging, mild cognitive impairment, and Alzheimer's disease. *Alzheimers Dement*. 2017;13(5):510–9. <https://doi.org/10.1016/j.jalz.2016.09.003>.
70. Barthelsson K, Pederson SM, Newman M, Lardelli M. Brain transcriptome analysis reveals subtle effects on mitochondrial function and iron homeostasis of mutations in the SORL1 gene implicated in early onset familial Alzheimer's disease. *Mol Brain*. 2020;13(1):142. <https://doi.org/10.1186/s13041-020-00681-7>.
71. Wong BX, et al. beta-Amyloid precursor protein does not possess ferroxidase activity but does stabilize the cell surface ferrous iron exporter ferroportin. *PLoS One*. 2014;9(12):e114174.
72. Yambire KF, Rostovsky C, Watanabe T, Pacheco-Grau D, Torres-Odio S, Sanchez-Guerrero A, Senderovich O, Meyron-Holtz EG, Milosevic I, Frahm J, West AP, Raimundo N. Impaired lysosomal acidification triggers iron deficiency and inflammation in vivo. *Elife*. 2019;8:e51031. <https://doi.org/10.7554/eLife.51031>.
73. Dlouhy AC, Bailey DK, Steimle BL, Parker HV, Kosman DJ. Fluorescence resonance energy transfer links membrane ferroportin, hephaestin but not ferroportin, amyloid precursor protein complex with iron efflux. *J Biol Chem*. 2019;294(11):4202–14. <https://doi.org/10.1074/jbc.RA118.005142>.
74. Ji CY, et al. The Ferroxidase Hephaestin but not amyloid precursor protein is required for Ferroportin-supported Iron efflux in primary hippocampal neurons. *Cell Mol Neurobiol*. 2018;38(4):941–54. <https://doi.org/10.1007/s10571-017-0568-z>.

75. Jiang Y, Sato Y, Im E, Berg M, Bordi M, Darji S, Kumar A, Mohan PS, Bandyopadhyay U, Diaz A, Cuervo AM, Nixon RA. Lysosomal dysfunction in down syndrome is APP-dependent and mediated by APP-beta CTF (C99). *J Neurosci*. 2019;39(27):5255–68. <https://doi.org/10.1523/JNEUROSCI.0578-19.2019>.
76. Pelegri F. Maternal factors in zebrafish development. *Dev Dyn*. 2003;228(3): 535–54. <https://doi.org/10.1002/dvdy.10390>.
77. Edgar R, Domrachev M, Lash AE. Gene expression omnibus: NCBI gene expression and hybridization array data repository. *Nucleic Acids Res*. 2002; 30(1):207–10. <https://doi.org/10.1093/nar/30.1.207>.
78. Lindgreen S. AdapterRemoval: easy cleaning of next-generation sequencing reads. *BMC Res Notes*. 2012;5(1):337. <https://doi.org/10.1186/1756-0500-5-337>.
79. Yates AD, et al. Ensembl 2020. *Nucleic Acids Res*. 2019;48(D1):D682–8.
80. Dobin A, Davis CA, Schlesinger F, Drenkow J, Zaleski C, Jha S, Batut P, Chaisson M, Gingeras TR. STAR: ultrafast universal RNA-seq aligner. *Bioinformatics*. 2013;29(1):15–21. <https://doi.org/10.1093/bioinformatics/bts635>.
81. Liao Y, Smyth GK, Shi W. featureCounts: an efficient general purpose program for assigning sequence reads to genomic features. *Bioinformatics*. 2014;30(7):923–30. <https://doi.org/10.1093/bioinformatics/btt656>.
82. Hoffman GE, Schadt EE. variancePartition: interpreting drivers of variation in complex gene expression studies. *BMC Bioinformatics*. 2016;17:483.
83. Robinson MD, McCarthy DJ, Smyth GK. edgeR: a bioconductor package for differential expression analysis of digital gene expression data. *Bioinformatics*. 2010;26(1):139–40. <https://doi.org/10.1093/bioinformatics/btp616>.
84. McCarthy DJ, Chen YS, Smyth GK. Differential expression analysis of multifactor RNA-Seq experiments with respect to biological variation. *Nucleic Acids Res*. 2012;40(10):4288–97. <https://doi.org/10.1093/nar/gks042>.
85. Slenter DN, Kutmon M, Hanspers K, Riutta A, Windsor J, Nunes N, Mélius J, Cirillo E, Coort SL, Digles D, Ehrhart F, Giesbertz P, Kalafati M, Martens M, Miller R, Nishida K, Rieswijk L, Waagmeester A, Eijssen LMT, Evelo CT, Pico AR, Willighagen EL. WikiPathways: a multifaceted pathway database bridging metabolomics to other omics research. *Nucleic Acids Res*. 2018; 46(D1):D661–7. <https://doi.org/10.1093/nar/gkx1064>.
86. Carlson, M., org. Dr.eb.db: Genome wide annotation for Zebrafish. 2017: R package version 3.5.0.
87. Young MD, et al. Gene ontology analysis for RNA-seq: accounting for selection bias. *Genome Biol*. 2010;11(2):R14.
88. Subramanian A, Tamayo P, Mootha VK, Mukherjee S, Ebert BL, Gillette MA, Paulovich A, Pomeroy SL, Golub TR, Lander ES, Mesirov JP. Gene set enrichment analysis: a knowledge-based approach for interpreting genome-wide expression profiles. *Proc Natl Acad Sci U S A*. 2005;102(43):15545–50. <https://doi.org/10.1073/pnas.0506580102>.
89. Sergushichev A. An algorithm for fast preranked gene set enrichment analysis using cumulative statistic calculation. *bioRxiv*. 2016. <https://doi.org/10.1101/060012>.
90. Campillos M, et al. SIREs: searching for iron-responsive elements. *Nucleic Acids Res*. 2010;38(Web Server issue):W360–7.
91. Carlson M. org. Dr.eb.db: Genome wide annotation for Zebrafish. R package version 3.8.2; 2019.
92. Liberzon A, Birger C, Thorvaldsdóttir H, Ghandi M, Mesirov JP, Tamayo P. The molecular signatures database (MSigDB) hallmark gene set collection. *Cell Syst*. 2015;1(6):417–25. <https://doi.org/10.1016/j.cels.2015.12.004>.
93. Kanehisa M, Goto S. KEGG: Kyoto encyclopedia of genes and genomes. *Nucleic Acids Res*. 2000;28(1):27–30. <https://doi.org/10.1093/nar/28.1.27>.
94. Dolgalev I. msigdb: MSigDB gene sets for multiple organisms in a tidy data format; 2020.

Publisher's Note

Springer Nature remains neutral with regard to jurisdictional claims in published maps and institutional affiliations.

Ready to submit your research? Choose BMC and benefit from:

- fast, convenient online submission
- thorough peer review by experienced researchers in your field
- rapid publication on acceptance
- support for research data, including large and complex data types
- gold Open Access which fosters wider collaboration and increased citations
- maximum visibility for your research: over 100M website views per year

At BMC, research is always in progress.

Learn more biomedcentral.com/submissions

